Copy No. 16

DEFENCE R&D DÉFENSE

THE PERFORMANCE OF THE ARCTANGENT BEARING ESTIMATOR IN ISOTROPIC NOISE

B.H. Maranda

DEFENCE RESEARCH ESTABLISHMENT ATLANTIC

Technical Memorandum

DREA TM 1999-145

September 1999

National Defence Défense nationale

Canada

National Defence
Research and Development Branch

Défense nationale
Bureau de recherche et développement

DREA TM 1999/145

The Performance of The Arctangent Bearing Estimator In Isotropic Noise

B.H. Maranda

DEFENCE RESEARCH ESTABLISHMENT
PO Box 1012, Dartmouth
Nova Scotia, Canada
B2Y 3Z7

Approved by: _____
I.A. Fraser
Group Leader/Sonar signal Processing

September 1999

TECHNICAL MEMORANDUM

Prepared by

Defence Research Establishment Atlantic

Centre de Recherches pour la Défense Atlantique

Canada

ABSTRACT

One well-known system for estimating the bearing to an underwater acoustic source consists of two crossed dipoles and an omni-directional hydrophone. The bearing is computed from the sensor data using an estimator based on the arctangent function. In this paper, the performance of the arctan bearing estimator is examined for a sinusoidal signal in isotropic Gaussian noise. It is shown analytically that the estimator is unbiased, and an exact formula for the bearing variance is derived; this formula is valid for an arbitrary number of data blocks and arbitrary values of the signal-to-noise ratio (SNR). Numerical examples show that the variance of the arctan estimator approaches the Cramér-Rao lower bound for high SNRs, and the threshold region below which the bearing accuracy rapidly degrades is clearly identified. Two different strategies are compared for averaging multiple data blocks while forming the bearing estimate.

RÉSUMÉ

Un système bien connu servant à l'estimation du gisement d'une source acoustique sous-marine est constitué de deux dipôles croisés et d'un hydrophone omnidirectionnel. Le gisement est calculé à partir des données de capteur à l'aide d'un estimateur basé sur la fonction arctangente. Dans la présente communication, la performance de l'estimateur de gisement à fonction arctg est examinée dans le cas d'un signal sinusoïdal en condition de bruit gaussien isotrope. On démontre par méthode analytique que l'estimateur n'est pas biaisé, et on établit pour la variance du gisement une formule exacte qui est valide pour un nombre arbitraire de blocs de données et des valeurs arbitraires du rapport signal-sur-bruit. Des exemples numériques montrent que la variance de l'estimateur à fonction arctg s'approche de la borne inférieure de Cramér-Rao pour les rapports signal-sur-bruit élevés, et la région seuil au-dessous de laquelle la précision du gisement se détériore rapidement est nettement définie. On compare deux stratégies différentes d'établissement de la moyenne pour des blocs de données multiples lorsqu'on produit l'estimation du gisement.

EXECUTIVE SUMMARY

TITLE

The Performance of the Arctangent Bearing Estimator in Isotropic Noise

AUTHOR

Brian H. Maranda

REPORT NUMBER

DREA Technical Memorandum 1999–145

INTRODUCTION

One well-known system for estimating the bearing to an underwater acoustic source consists of two crossed dipoles and an omni-directional hydrophone. The bearing is computed from the sensor data using an estimator based on the arctangent function. Previous investigations of the bearing accuracy attained in the presence of noise have employed approximations that restrict the range of parameters over which the results are valid.

PRINCIPAL RESULTS

The main result of this investigation is an exact formula for the error of the above system when estimating the bearing of a narrowband signal in isotropic Gaussian noise. The formula is completely general in nature, holding for an arbitrary number of data blocks and arbitrary values of the signal-to-noise ratio (SNR). Furthermore, it can be evaluated very efficiently on a digital computer. Numerical examples computed using this formula show that, when the SNR is high, the variance of the arctan bearing estimator approaches the theoretical minimum, as given by the Cramér-Rao lower bound (CRLB). The simple formula for CRLB can therefore be used to approximate the variance at high SNR. Finally, it is demonstrated that the averaging of multiple data blocks should take place before, and not after, the application of the arctangent function.

SIGNIFICANCE OF RESULTS

(1) The formula for the bearing error derived herein is a useful tool for examining the error of the arctan bearing estimator without having to carry out time-consuming computer simulations. (2) Since the arctan bearing estimator achieves the minimum possible variance at high SNRs, no improvements are possible in this regime, at least for a single target in isotropic noise. (3) It is important to perform the averaging of multiple data blocks in the correct way if the useful range of the estimator is to be extended to lower SNRs.

SUGGESTIONS FOR FUTURE WORK

It would be worthwhile to compare the results for the sinsoidal-signal model used in this paper with the Gaussian-signal model used in previous studies.

TABLE OF CONTENTS

ABSTRACT ii
EXECUTIVE SUMMARY iii
TABLE OF CONTENTS iv
1. INTRODUCTION 1
2. THE SIGNAL AND NOISE MODEL 1
    2.1 A Single Data Block 1
    2.2 The Cramér-Rao Lower Bound 4
    2.3 Extension to Multiple Data Blocks 5
3. THE ARCTAN BEARING ESTIMATOR 6
    3.1 Introduction 6
    3.2 Analytical Results 6
    3.3 Numerical Examples 7
        3.3.1 Constant SNR per Block 7
        3.3.2 Constant SNR Over Entire Data Record 10
        3.3.3 Averaging After the Arctangent 10
4. SUMMARY AND DISCUSSION 12
APPENDIX A: ANALYSIS OF THE ARCTAN ESTIMATOR 14
    A.1 Analysis for a Single Data Block 14
    A.2 Extension to Multiple Data Blocks 17
    A.3 Evaluation of the Inner Integral 20
APPENDIX B: HIGH-SNR APPROXIMATION FOR THE ERROR 22
REFERENCES 24

1. INTRODUCTION

One well-known system for estimating the bearing to an underwater acoustic source consists of two crossed dipoles and an omni-directional hydrophone. This arrangement is used, for example, in the DIFAR sonobuoy. The total bearing error in such a system is a combination of errors caused by many different effects. Most of the error components are independent of the acoustic signals, depending instead on the system hardware; hence, they can be reduced through improvements in system construction. However, there is an unavoidable bearing error induced by the component of ambient ocean noise that is present in the acoustic signals. This noise places an ultimate limitation on the achievable bearing accuracy and can often be the dominant source of error.

Some analysis has been done at DREA on determining the variance of the bearing error for a specific bearing estimator based on the arctangent function[1-3]. In these studies the signal and noise were assumed to have Gaussian statistics, and the noise was taken to be spatially isotropic. Merklinger[1] found an approximation for the bearing error that is valid at high signal-to-noise ratios; only a single data block was treated. Davies[3] noted the difficulty of deriving an exact expression for the bearing error, and used an approximate approach based on the central limit theorem. His approximate results are valid only when a large number of data blocks are integrated before forming the bearing estimate; for example, by using computer simulations he found that his analytical approximation is good only to an accuracy of 20% when 40 blocks are averaged.

In this paper, the performance of the arctan bearing estimator is examined for a sinusoidal signal in isotropic Gaussian noise. It is shown analytically that the estimator is unbiased, and an exact formula for the bearing error (variance) is derived. The formula holds for an arbitrary number of data blocks; furthermore, it is valid for an arbitrary signal-to-noise ratio, thereby allowing an accurate investigation of threshold effects to be made. Several illustrative examples based on the numerical evaluation of the bearing variance are presented; for example, the bearing variance of the arctan estimator is compared with the minimal attainable variance as given by the Cramér-Rao lower bound.

Although the results in the paper are stated for the case when multiple data blocks are processed, much of the theoretical development is given for a single data block with only a brief explanation of how the result is extended to multiple blocks. In this way the basic argument is not obscured by a proliferation of notation. Also, most of the detailed analytical work is relegated to Appendices.

2. THE SIGNAL AND NOISE MODEL

2.1 A Single Data Block

As a first step in the analysis, a model will be derived for the signal and noise received by the three sensor channels, which are arranged as shown in Fig. 1. The subscripts o, c, and s will be used to designate the omni, cosine, and sine channels. Analog signals and processing will be assumed throughout the analysis as a matter of convenience; the

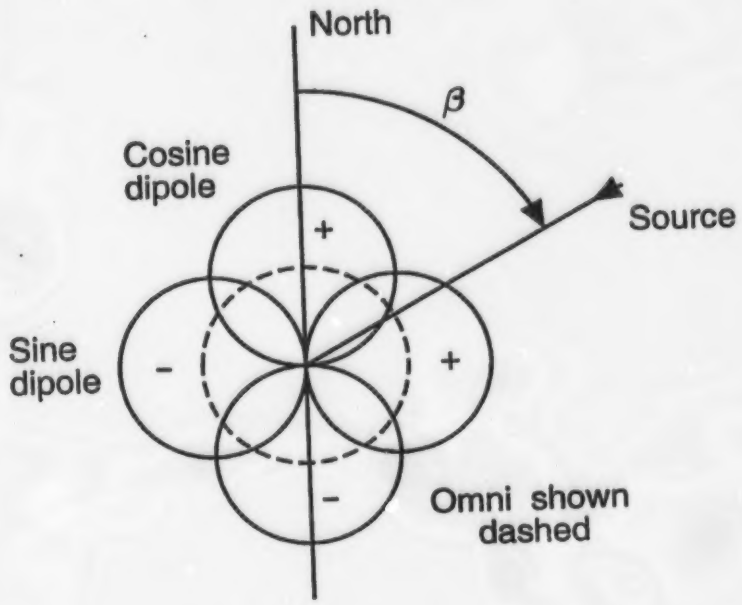

Figure 1. Geometric arrangement of the three sensors.

results would be the same for the equivalent digital processing. It will be assumed that there is a single source producing a narrowband signal of the form

$$y(t) = 2B\cos(\nu t + \psi), \tag{1}$$

where $2B$ is the amplitude, ν the frequency, and ψ an arbitrary phase. The amplitude has been written as $2B$ to simplify the subsequent equations. When the source is at bearing β, the sensors produce the waveforms

$$\begin{aligned} x_o(t) &= y(t) + n_o(t) \\ x_c(t) &= y(t)\cos\beta + n_c(t) \\ x_s(t) &= y(t)\sin\beta + n_s(t), \end{aligned} \tag{2}$$

where $n_o(t)$, $n_c(t)$, and $n_s(t)$ are the noise components. As noted in the introduction, the noise components are assumed to arise from ambient ocean noise.

The input data to the bearing estimator will be the Fourier coefficients of the waveforms in Eq. (2). Since the signals are observed for a finite time, the Fourier transform of an arbitrary signal $f(t)$ will be defined by

$$F(\omega) = \frac{1}{T}\int_0^T f(t)e^{-i\omega t}dt, \tag{3}$$

where T is the observation time, or record length. For simplicity, it will be assumed that the transforms are taken exactly at the frequency of the sinusoidal signal; i.e., $\omega = \nu$. From Eqs. (1) and (3), it is found that

$$Y(\nu) = B\left\{e^{i\psi} + e^{-i(\nu T+\psi)}\frac{\sin(\nu T)}{\nu T}\right\},$$

where, as in Eq. (3), the capital letter Y is used to denote the Fourier transform of the corresponding lower-case signal $y(t)$. If it is assumed that $\nu T \gg 1$, then to a high degree of approximation

$$Y \cong Be^{i\psi}. \tag{4}$$

In other words, it will be assumed that the second term falls into the sidelobe region of the rectangular window, and can therefore be neglected. This approximation is often made in the Fourier analysis of narrowband signals; see, for example, Ref. 4. After Fourier transformation, Eqs. (2) can be written in the vector form $\mathbf{x} = \mathbf{y} + \mathbf{n}$ with

$$\mathbf{x} = \begin{pmatrix} X_o \\ X_c \\ X_s \end{pmatrix}, \quad \mathbf{y} = Be^{i\psi}\begin{pmatrix} 1 \\ \cos\beta \\ \sin\beta \end{pmatrix}, \quad \text{and} \quad \mathbf{n} = \begin{pmatrix} N_o \\ N_c \\ N_s \end{pmatrix}. \tag{5}$$

Here $X_o = X_o(\nu)$, etc.

The noise will be assumed to have Gaussian statistics, which are completely determined by the values of the mean and covariance. The mean is taken to be zero; i.e., $E\{\mathbf{n}\} = \mathbf{0}$. It remains to specify the covariance matrix, given by $\mathbf{K} \equiv E\{\mathbf{n}\mathbf{n}^\dagger\}$, where the dagger denotes the transpose conjugate. The only noise distributions considered will be 2D- and 3D-isotropic noise, for which the covariance matrix assumes the simple form

$$\mathbf{K} = \sigma^2\begin{pmatrix} 1 & 0 & 0 \\ 0 & \gamma & 0 \\ 0 & 0 & \gamma \end{pmatrix}, \tag{6}$$

where $\sigma^2 \equiv E\{|N_o|^2\}$ is the noise power in the Fourier bin of the omni channel and γ is the noise gain of either dipole. The value of $\gamma = 1/2$ or $1/3$ for 2D-isotropic or 3D-isotropic noise respectively[3]. All the off-diagonal terms of $\mathbf{K}$ are zero for isotropic noise; it is this simplicity that makes the rest of the analysis tractable.

We shall denote by ρ the signal-to-noise ratio (SNR) in the Fourier bin of the omni channel. The signal component in the bin is given by Eq. (4), and we have

$$\rho = \frac{|Y|^2}{E\{|N_o|^2\}} = \frac{B^2}{\sigma^2}.$$

The SNR in the bin can be related to the input quantities as follows. First, the average power of the signal in Eq. (1) is $P_s = \frac{1}{2}(2B)^2 = 2B^2$. Also, if the noise $n_o(t)$ recorded

by the omni sensor is white with two-sided power spectral density $\eta/2$, then it can be shown from Eq. (3) that $\sigma^2 = \eta/2T$. Hence the SNR as defined above is equal to

$$\rho = \frac{P_s T}{\eta} = \frac{P_s}{\eta W},$$

where $W = 1/T$ is the nominal bandwidth of the Fourier analysis cell. In words, the SNR is given by the ratio of the average signal power to the average noise power entering into the bin. If the time functions are weighted before the Fourier transform is performed, the SNR is reduced by the equivalent noise bandwidth of the weighting function.

2.2 The Cramér-Rao Lower Bound

Suppose that we have received a vector $\mathbf{x}$ of stochastic measurements depending on a vector of parameters $\boldsymbol{\theta} = (\theta_1, \theta_2, \ldots)^T$ and form estimates of the parameters on the basis of this received data. If the conditional density function $p(\mathbf{x}|\boldsymbol{\theta})$ is known, and if the estimates are unbiased, then their variance can be bounded below by the Cramér-Rao lower bound[5]. To compute the CRLB we first form the Fisher information matrix $\mathbf{J}$, the (p,q)-th element of which is given by

$$J_{pq} \equiv -E\left\{\frac{\partial^2}{\partial\theta_p \partial\theta_q} \log p(\mathbf{x}|\boldsymbol{\theta})\right\}, \tag{7}$$

where the expectation $E\{\cdot\}$ is taken with respect to $p(\mathbf{x}|\boldsymbol{\theta})$. Letting J^{pq} denote the (p,q)-th element of the inverse $\mathbf{J}^{-1}$ of the Fisher information matrix, the CRLB on the variance of any unbiased estimator $\hat{\theta}_p$ of the parameter θ_p is given by $\sigma^2_{\hat{\theta}_p} \geq J^{pp}$.

For the model developed in §2.1, the data $\mathbf{x}$ obey a complex Gaussian distribution of the form

$$p(\mathbf{x}|\boldsymbol{\theta}) = \frac{1}{\pi^3 \det \mathbf{K}} \exp[-(\mathbf{x}-\mathbf{y})^\dagger \mathbf{K}^{-1} (\mathbf{x}-\mathbf{y})].$$

It may be shown that, in this special case, the elements of the Fisher matrix as given by Eq. (7) are equal to

$$J_{pq} = \mathrm{tr}\left\{\mathbf{K}^{-1}\frac{\partial \mathbf{K}}{\partial\theta_p}\mathbf{K}^{-1}\frac{\partial \mathbf{K}}{\partial\theta_q}\right\} + 2\,\mathrm{Re}\left\{\frac{\partial \mathbf{y}^\dagger}{\partial\theta_p}\mathbf{K}^{-1}\frac{\partial \mathbf{y}}{\partial\theta_q}\right\}, \tag{8}$$

where $\mathrm{tr}\{\cdot\}$ denotes the matrix trace operation*. For the problem at hand, we set $\boldsymbol{\theta} = (\theta_1, \theta_2, \theta_3)^T = (B, \psi, \beta)^T$. The covariance matrix $\mathbf{K}$ is independent of the parameters, and so only the last term in Eq. (8) contributes to the Fisher information matrix; the result is

$$\mathbf{J} = \frac{2}{\sigma^2}\begin{pmatrix} 1+\gamma^{-1} & 0 & 0 \\ 0 & B^2(1+\gamma^{-1}) & 0 \\ 0 & 0 & B^2/\gamma \end{pmatrix}.$$

* Scharf[5] derives the formula for the case when the variables are real-valued.

All the off-diagonal entries of $\mathbf{J}$ are zero, meaning that there is no interaction between parameters. The inverse of the matrix is found simply by inverting each entry along the diagonal, whence it follows that the variance of any unbiased bearing estimator obeys the bound

$$\sigma_{\hat{\beta}}^2 \geq \frac{\sigma^2 \gamma}{2B^2} = \frac{\gamma}{2\rho}. \tag{9}$$

The lower bound is inversely proportional to the SNR ρ.

2.3 Extension to Multiple Data Blocks

The previous development has been for a single data block. The signal-and-noise model in Eq. (5) is now extended to handle the case of multiple blocks by allowing the observation to consist of M data vectors $\mathbf{x}_m = \mathbf{y}_m + \mathbf{n}_m$, where

$$\mathbf{x}_m = \begin{pmatrix} X_{o,m} \\ X_{c,m} \\ X_{s,m} \end{pmatrix}, \quad \mathbf{y}_m = B_m e^{i\psi_m} \begin{pmatrix} 1 \\ \cos\beta \\ \sin\beta \end{pmatrix}, \quad \text{and} \quad \mathbf{n}_m = \begin{pmatrix} N_{o,m} \\ N_{c,m} \\ N_{s,m} \end{pmatrix}. \tag{10}$$

It will be assumed that noise from the different blocks is independent; this requirement implies, for example, that there cannot be any overlap of the input data records before Fourier transformation. Note that the bearing β is assumed to be the same for all data blocks, an assumption that may place constraints on the allowable integration time. The amplitudes B_m and phases ψ_m will be treated as unknown but deterministic constants; that is, they have no associated probability distributions.

Deriving the CRLB on the variance $\sigma_{\hat{\beta}}^2$ is not much more difficult for the extended model (10) than it was for the model (5). There are now $2M+1$ parameters which must enter into the Fisher information matrix: the M amplitudes B_m, the M phases ψ_m, and the bearing β. The SNR for the mth block will be defined by $\rho_m = B_m^2/\sigma^2$, and the SNR for the entire data record by

$$\rho = \frac{\|\mathbf{b}\|^2}{\sigma^2} = \sum_{m=1}^{M} \rho_m \,, \tag{11}$$

where $\mathbf{b} = (B_1, \ldots, B_M)^T$ is the vector of signal amplitudes and $\|\cdot\|$ denotes the Euclidean norm. It will be stated without proof that the CRLB on the variance of $\hat{\beta}$ is

$$\sigma_{\hat{\beta}}^2 \geq \frac{\gamma}{2\rho} \tag{12}$$

as in Eq. (9), but with ρ now given by Eq. (11).

3. THE ARCTAN BEARING ESTIMATOR

3.1 Introduction

We now consider the performance of a specific bearing estimator called the arctan estimator, which is defined as follows: given the frequency-domain data of Eq. (10), we first compute

$$\begin{aligned} \hat{c} &= \mathrm{Re} \sum_{m=1}^{M} X_{c,m} X_{o,m}^{*} \\ \hat{s} &= \mathrm{Re} \sum_{m=1}^{M} X_{s,m} X_{o,m}^{*}, \end{aligned} \tag{13}$$

and then form a bearing estimate using the equation

$$\hat{\beta} = \arctan(\hat{s}/\hat{c}). \tag{14}$$

One can easily see from the previous definitions that at high SNR, $\hat{c}$ and $\hat{s}$ are approximately $\|\mathbf{b}\|^2 \cos\beta$ and $\|\mathbf{b}\|^2 \sin\beta$ respectively, and so the definition of Eq. (14) makes intuitive sense.

Although the arctan bearing estimator is usually written as in Eq. (14), the ratio $\hat{s}/\hat{c}$ is alone insufficient to form a bearing estimate, because it is necessary to know the signs of $\hat{s}$ and $\hat{c}$ in order to determine the correct quadrant. More precisely, $\hat{\beta}$ is determined from the polar transformation

$$\begin{aligned} \hat{c} &= \hat{r} \cos\hat{\beta} \\ \hat{s} &= \hat{r} \sin\hat{\beta}, \end{aligned} \tag{15}$$

where $\hat{r}$ is positive and $\hat{\beta}$ is chosen to lie in an interval of length 2π. Here $\hat{r}$ can be used to estimate $\|\mathbf{b}\|^2$, an application that will not be considered further.

3.2 Analytical Results

The analysis of the arctan bearing estimator is long and can be found in Appendix A; only the main results are cited here. First, the arctan estimator is unbiased. Hence, its variance may be compared directly with the CRLB, which assumes an unbiased estimator. Furthermore, an exact formula for the variance is given by

$$\begin{aligned} \sigma_{\hat{\beta}}^2 = \frac{\rho^M e^{-\rho}}{\sqrt{\pi}\,\Gamma(M-\frac{1}{2})} \int_{-\pi}^{\pi} K\Big(\sqrt{\tfrac{\rho}{\gamma}}\cos\theta\Big) \sin^{2M-2}\theta \\ \times \int_0^{\infty} \exp\big[-\rho(t^2 - 2t\cos\theta)\big] t^{2M-1}\, dt\, d\theta, \end{aligned} \tag{16}$$

where $K(\cdot)$ is an auxiliary function defined by the double integral

$$K(x) = \frac{1}{\pi} \int_{-\pi}^{\pi} \int_0^{\infty} \theta^2 \exp\big[-(x^2 + t^2 - 2xt\cos\theta)\big] t\, dt\, d\theta. \tag{17}$$

This last function is not a standard function of analysis.

Equations (16) and (17) appear formidable, and it is worthwhile to pause and consider the various terms involved. First, a number of analytical representations can derived for the function $K(\cdot)$, such as its power series and asymptotic expansions. In this paper, it will be taken for granted that $K(\cdot)$ can be evaluated on the computer with speed and accuracy using these expansions*. Second, the inner integral in Eq. (16),

$$\int_0^\infty \exp\left[-\rho(t^2 - 2t\cos\theta)\right] t^{2M-1}\, dt,$$

can be expressed in terms of the Gaussian distribution function. However, the analytical expressions become progressively more complicated as the value of M increases, and purely numerical methods must be sought for large values. As is discussed in Appendix A, the integral can be evaluated for arbitrary M using a recursion relation. Thus, only the outer integral in Eq. (16) need be done by numerical quadrature; high speed and accuracy can consequently be attained in the numerical evaluation of the estimator variance.

3.3 Numerical Examples

We now present several numerical examples. There are too many parameters to allow an exhaustive examination of how they affect bearing accuracy, and in the examples to follow only a few simple cases will be worked through. Formula (16) was used for evaluating the variance of the arctan estimator in all cases, except where noted otherwise. The parameter γ was set to 1/3, corresponding to 3D-isotropic noise.

3.3.1 Constant SNR per Block

We consider the case when the SNR per block has the constant value $\rho_m = \rho_b$, yielding $\rho = \sum_m \rho_m = M\rho_b$. Figure 2 shows $\sigma_{\hat{\beta}}$ as a function of ρ_b for different values of M; the upper plot shows $\sigma_{\hat{\beta}}$ over a wide range of parameters and the lower plot in a range of more interest for practical applications. Indicated by the circles in Fig. 2 are the results of a Monte Carlo simulation for the case $M = 8$. The agreement with the theoretical curve is excellent†. However, the numerical evaluation of $\sigma^2_{\hat{\beta}}$ via Eq. (16), in addition to being more accurate than a Monte Carlo simulation, is computationally more efficient: on an SGI Indigo, a few seconds sufficed to compute the 161 points used to draw each theoretical curve in Fig. 2(a), whereas many minutes were required to compute each of the simulated-data points.

As can be seen from Fig. 2(a), the bearing error rises steeply when ρ_b drops below a value in the range 0 to 10 dB, depending on the value of M. Behavior of this

* The derivation of the expansions and their use in numerically evaluating the function will be the topic of a separate paper.

† The simulation was based on the signal and noise model of Eq. (10), in which the edge effect of the FFT has been neglected.

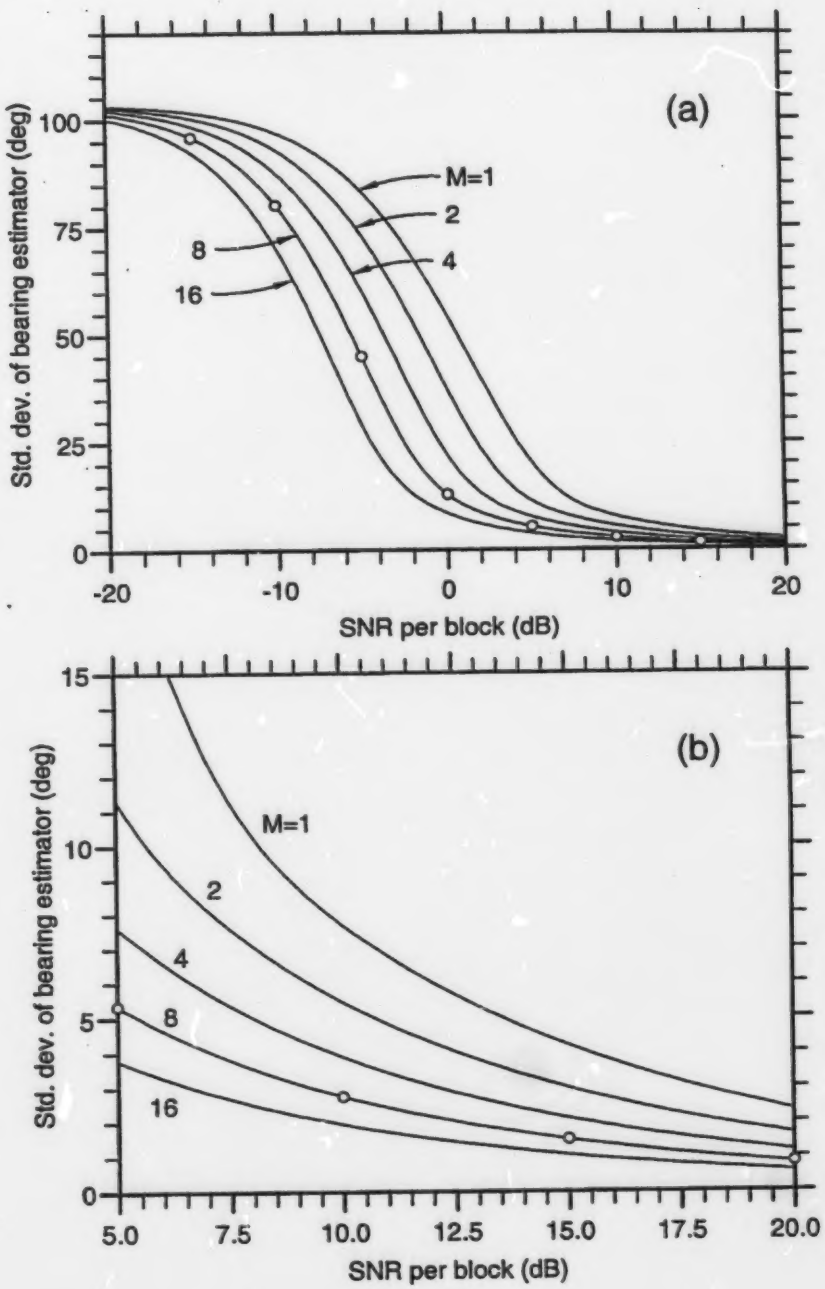

Figure 2. Standard deviation of the arctan bearing estimator versus the per-block SNR, ρ_b, for different numbers of data blocks, M. Circles indicate simulated data points. Plots (a) and (b) differ only in their axes.

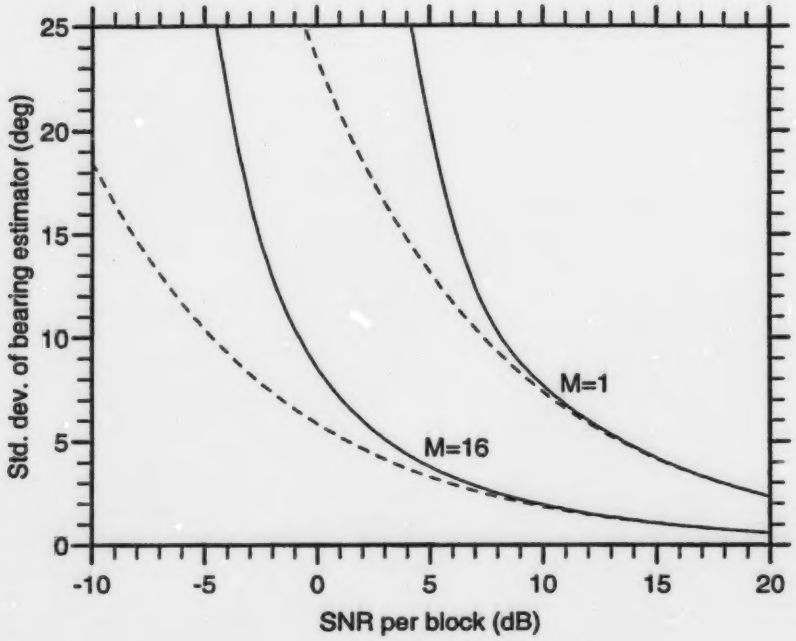

Figure 3. The standard deviation of the arctan estimator (solid lines) compared with the Cramér-Rao lower bound (dashed lines).

type is referred to as a threshold effect and often occurs with non-linear estimators (of which the arctan bearing estimator is one). By integrating more blocks, we extend the useful SNR range of the estimator. For very low SNRs the pdf of $\hat{\beta}$ is approximately uniform, regardless of the value of M, and a simple calculation shows that $\sigma_{\hat{\beta}} \to 103.9°$ asymptotically.

Figure 3 replots the standard deviation for $M = 1$ and 16, and also shows the Cramér-Rao lower bound for the two cases. It is seen that the bearing error asymptotically approaches the CRLB at high SNRs; in statistical terminology, the arctan bearing estimator is efficient. The CRLB results can also be used to assign a more definite value to the threshold SNR, which the author would place between 5 and 10 dB on the basis of Fig. 3. When the arctan bearing estimator is operating above threshold, it follows from Eq. (12) that its standard deviation can be estimated accurately using the simple formula

$$\sigma_{\hat{\beta}} \cong \sqrt{\frac{\gamma}{2\rho}}, \tag{18}$$

where $\rho = \sum_m \rho_m$. In the case $M = 1$, the high-SNR approximation in Eq. (18) can also be derived directly from the signal-and-noise model in Eq. (5); see Appendix B.

3.3.2 Constant SNR Over Entire Data Record

In the previous case, the signal energy was the same for each block. The total signal energy grew in direct proportion to M, and hence the bearing variance decreased as more blocks were added. Let us now view the processing from a different perspective: suppose we work with one fixed-energy data block, dividing it into M sub-blocks. In this case, ρ remains constant as M is varied, and the per-block value $\rho_b = \rho/M$ decreases as M is increased. Because the total signal energy remains constant, we observe only the effect of breaking the main data record into sub-blocks.

Figure 4 shows curves of $\sigma_{\hat{\beta}}$ as a function of ρ for different values of M. Since we have the relationship

$$10 \log \rho = 10 \log \rho_b + 10 \log M$$

connecting ρ and ρ_b, each curve in Fig. 4 can be found by shifting the corresponding curve in Fig. 2 to the right by a value $10 \log M$. It is seen that sub-dividing the data block while holding the total energy constant degrades the performance of the bearing estimator. This behavior is not surprising, since the coherent integration time decreases as the number of sub-blocks is increased. It is concluded that the block length should be chosen as large as possible; the constraint in practice will be the coherence time of the signal.

3.3.3 Averaging After the Arctangent

An alternative method of forming a bearing estimate from multiple blocks is to compute a bearing $\hat{\beta}_m$ for the mth block using the arctan estimator, and then average the individual estimates. Using a prime to distinguish this second estimator from the one defined earlier in Eqs. (13) and (14), we may write

$$\hat{\beta}' = \frac{1}{M} \sum_{m=1}^{M} \hat{\beta}_m, \tag{19}$$

where

$$\hat{\beta}_m \equiv \arctan \left[\frac{\mathrm{Re}\{X_{s,m} X_{o,m}^*\}}{\mathrm{Re}\{X_{c,m} X_{o,m}^*\}} \right]. \tag{20}$$

The estimators $\hat{\beta}$ and $\hat{\beta}'$ differ in whether integration takes place before or after the arctan function is applied; for convenience, we shall say that the first estimator uses pre-bearing integration and the second post-bearing integration[3].

For the signal and noise model of this paper, the random variables $\hat{\beta}_m$ in Eq. (20) are independent and identically distributed; it then follows from Eq. (19) that

$$\sigma_{\hat{\beta}'}^2 = \frac{1}{M^2} \sum_m \sigma_{\hat{\beta}_m}^2.$$

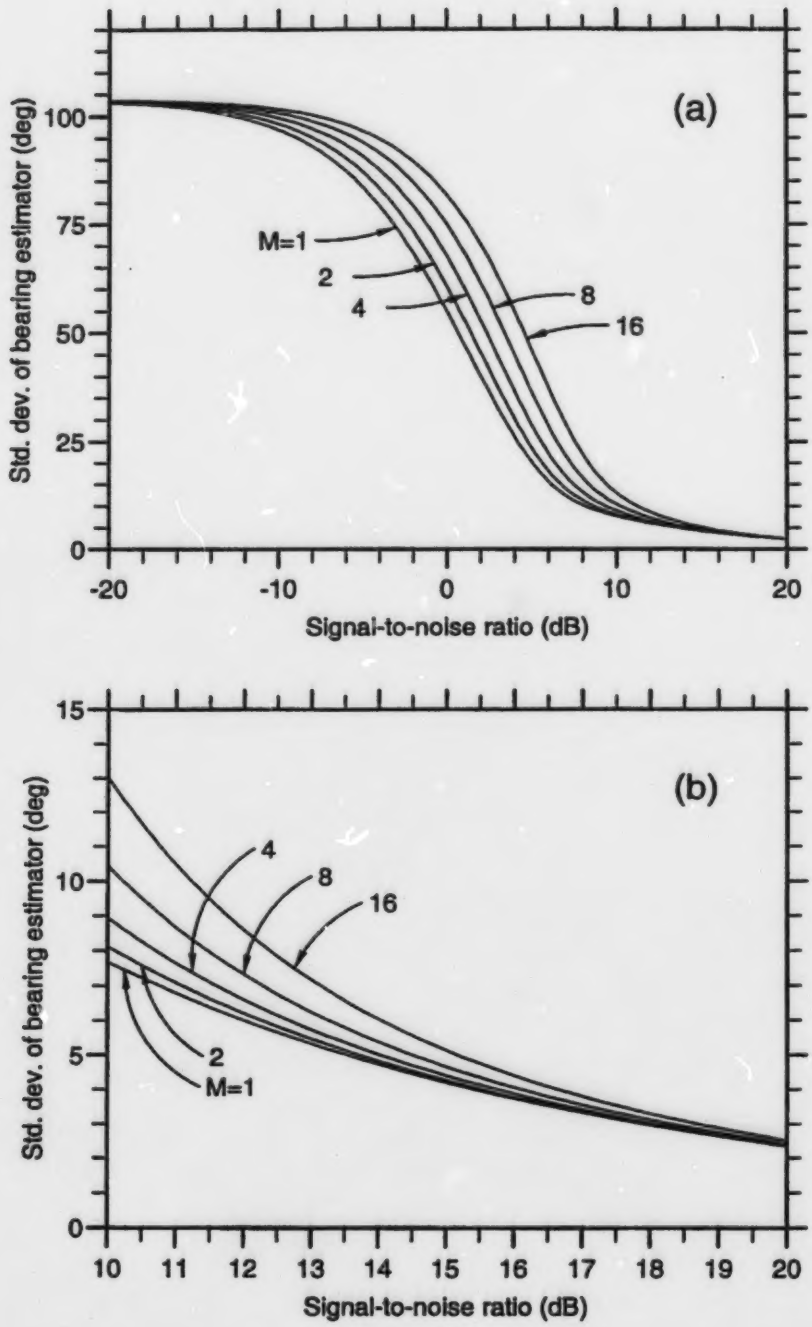

Figure 4. Standard deviation of the arctan bearing estimator versus the SNR, ρ, for different numbers of data blocks, M. Plots (a) and (b) differ only in their axes.

When the block SNRs ρ_m are all high, we have $\sigma^2_{\hat{\beta}_m} \cong \gamma/2\rho_m$ and

$$\sigma_{\hat{\beta}'} \cong \sqrt{\frac{\gamma}{2\rho'}}, \tag{21}$$

where an equivalent SNR has been defined for $\hat{\beta}'$ by

$$\rho' \equiv \frac{M^2}{\sum_m \rho_m^{-1}}.$$

A comparison of Eqs. (18) and (21) shows that, in the high-SNR region, any performance difference between pre- and post-bearing integration stems solely from the difference in the values of ρ and ρ'. Now, it can be shown that $\rho \geq \rho'$ for arbitrary positive values of ρ_m, and hence pre-bearing integration will provide better performance in general. Equality holds when the ρ_m are all equal (constant SNR per block, as in §3.3.1 above).

It should be noted that "high SNR" does not have the same meaning for the two estimators $\hat{\beta}$ and $\hat{\beta}'$, since their threshold behavior is different. The first estimator is above threshold as long as the cumulative SNR $\rho = \sum_m \rho_m$ is sufficiently great, the distribution of the individual ρ_m being unimportant. As for $\hat{\beta}'$, each of its constituent estimators $\hat{\beta}_m$ must be above threshold for approximation (21) to be valid; hence, the threshold of $\hat{\beta}'$ is no better than that attained with a single data block. As an example, let us assume that the per-block SNR has the constant value $\rho_m = \rho_b$. The two estimators will then have the same performance at high SNR, but their thresholds will differ. This behavior is illustrated in Figure 5, which shows the curves for $M = 16$ plotted as a function of ρ_b. It is concluded that post-bearing integration cannot be recommended for the processing of multiple blocks; the same conclusion was reached by Davies[3].

4. SUMMARY AND DISCUSSION

The performance of an arctangent bearing estimator has been studied for a system consisting of crossed dipoles and a co-located omni-directional sensor. In particular, an exact formula has been derived for the variance of the bearing error induced by isotropic Gaussian noise when the signal is sinusoidal. The formula is valid for an arbitrary number of data blocks and arbitrary signal-to-noise ratios, thus allowing threshold effects to be readily examined without recourse to time-consuming simulations. Numerical examples showed that, at high SNR, the performance of the bearing estimator approaches the theoretical limit given by the Cramér-Rao lower bound. Comparison of the exact result with the CRLB also allowed the threshold region to be identified clearly. Averaging multiple data blocks extends the threshold to lower SNRs, but it is important that the averaging take place before the non-linearity (the arctan function) and not after.

In this study the signal was modelled as a sinusoid, whereas previous investigators have assumed a Gaussian signal. The model used here is appropriate when the source is

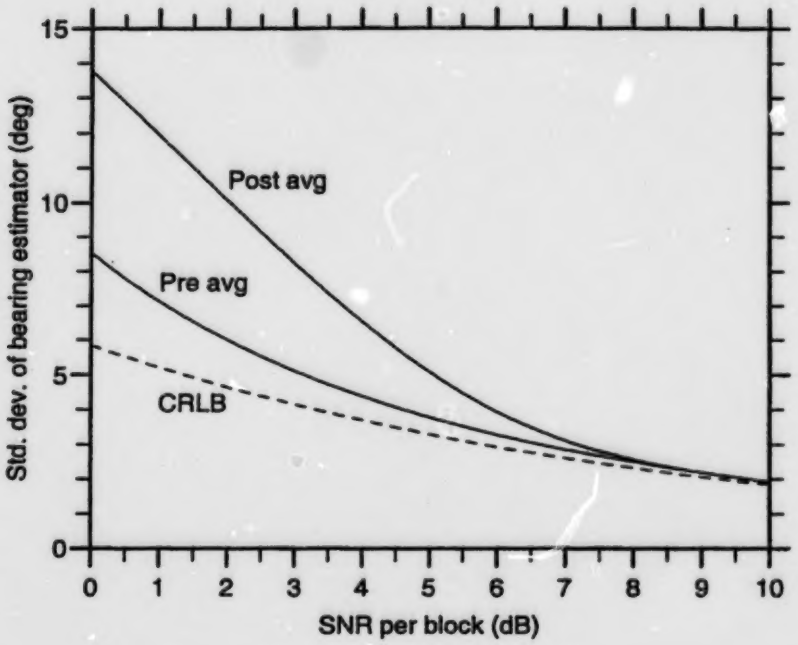

Figure 5. The effect of pre- and post-bearing integration on the accuracy of bearing estimation. The number of blocks is $M = 16$.

emitting a narrowband line, but the Gaussian model would be preferable when the signal is wideband. (In the first case, integration is usually performed in time, while in the second, integration can also be performed across frequency.) It would be worthwhile to compare the performance of the arctan estimator for the two different models. It may be possible to extend the exact formula for the sinusoidal signal to a Gaussian signal, and this will be an area of future research.

APPENDIX A: ANALYSIS OF THE ARCTAN ESTIMATOR

In this Appendix, the arctan bearing estimator is analyzed in detail. It is shown in what sense $\hat{\beta}$ is unbiased, and an explicit expression is derived for the variance $\sigma^2_{\hat{\beta}}$. For simplicity in exposition, an expression for $\sigma^2_{\hat{\beta}}$ is first found for a single data block ($M = 1$), and then extended to the general case of multiple blocks with only minimal explanation. Coordinate transformations that reduce the general result to a form suitable for numerical evaluation will be explained in detail.

A.1 Analysis for a Single Data Block

The method of analysis will be to derive the joint probability density function (pdf) of $\hat{c}$ and $\hat{s}$ in Eq. (13), from which the pdf $p(\hat{\beta})$ can be obtained by a polar transformation and an integration. Unfortunately, the number of variables is large and it is necessary to introduce more notation. We use the equation

$$\mathbf{x} = \begin{pmatrix} X_o \\ X_c \\ X_s \end{pmatrix} = \begin{pmatrix} a_1 + ia_2 \\ c_1 + ic_2 \\ s_1 + is_2 \end{pmatrix}$$

to define the variables on the right-hand side*. The six variables thus introduced are Gaussian and independent; their means can be deduced from Eq. (5) upon noting that $E\{\mathbf{x}\} = \mathbf{y}$, and their variances can be deduced from the covariance matrix $\mathbf{K}$. It will be useful for the subsequent derivation to define the two-dimensional vectors

$$\mathbf{a} = \begin{pmatrix} a_1 \\ a_2 \end{pmatrix}, \quad \mathbf{c} = \begin{pmatrix} c_1 \\ c_2 \end{pmatrix}, \quad \text{and} \quad \mathbf{s} = \begin{pmatrix} s_1 \\ s_2 \end{pmatrix},$$

whose means are given by

$$\mathbf{m}_a = B \begin{pmatrix} \cos\psi \\ \sin\psi \end{pmatrix}, \quad \mathbf{m}_c = B\cos\beta \begin{pmatrix} \cos\psi \\ \sin\psi \end{pmatrix}, \quad \text{and} \quad \mathbf{m}_s = B\sin\beta \begin{pmatrix} \cos\psi \\ \sin\psi \end{pmatrix}.$$

From the definition of $\hat{c}$ and $\hat{s}$ in Eq. (13) for $M = 1$, it follows that

$$\hat{c} = \mathbf{c}^T\mathbf{a} \qquad \text{and} \qquad \hat{s} = \mathbf{s}^T\mathbf{a}.$$

When it is convenient, we shall set $w_1 = \hat{c}$ and $w_2 = \hat{s}$, with corresponding vector $\mathbf{w} = (w_1, w_2)^T$. The difficulty in the analysis stems from the fact that a appears in the expressions for both $\hat{c}$ and $\hat{s}$, which are therefore statistically dependent. The statistical dependence will be handled by adapting a method that has been applied to a problem in

* The symbol a is used instead of o to denote the omni terms in order to avoid the usual confusion that arises between "oh" and "zero".

electrical communications[6]. The idea is that when the joint probability density function of $\hat{c}$ and $\hat{s}$ is conditioned on $\mathbf{a}$, this latter variable is considered constant. But $\hat{c}$ and $\hat{s}$ are independent when $\mathbf{a}$ is held constant (since $\mathbf{c}$ and $\mathbf{s}$ are independent), and their joint conditional pdf is therefore factorable:

$$p_{\hat{c},\hat{s}}(\mathbf{w}|\mathbf{a}) = p_{\hat{c}}(w_1|\mathbf{a})p_{\hat{s}}(w_2|\mathbf{a}).$$

The desired pdf $p_{\hat{c},\hat{s}}(\mathbf{w})$ is obtained by integrating over the density function $p(\mathbf{a})$ of $\mathbf{a}$, yielding the expression

$$p_{\hat{c},\hat{s}}(\mathbf{w}) = \iint_{-\infty}^{\infty} p_{\hat{c}}(w_1|\mathbf{a})p_{\hat{s}}(w_2|\mathbf{a})p(\mathbf{a})\,d\mathbf{a}, \tag{22}$$

where $d\mathbf{a} = da_1\,da_2$.

We now find explicit expressions for the probability density functions in Eq. (22). Considering $\hat{c} = \mathbf{c}^T\mathbf{a}$ when $\mathbf{a}$ is held constant, we see that it is the weighted sum of the two independent Gaussian random variables c_1 and c_2. Hence $\hat{c}$ is (conditionally) Gaussian, and it can be shown that

$$p_{\hat{c}}(w_1|\mathbf{a}) = \frac{1}{\sigma\|\mathbf{a}\|\sqrt{\pi\gamma}} \exp\left[-\frac{(w_1 - \mathbf{m}_c^T\mathbf{a})^2}{\gamma\sigma^2\|\mathbf{a}\|^2}\right].$$

Similarly,

$$p_{\hat{s}}(w_2|\mathbf{a}) = \frac{1}{\sigma\|\mathbf{a}\|\sqrt{\pi\gamma}} \exp\left[-\frac{(w_2 - \mathbf{m}_s^T\mathbf{a})^2}{\gamma\sigma^2\|\mathbf{a}\|^2}\right].$$

Lastly, we have that

$$p(\mathbf{a}) = \frac{1}{\pi\sigma^2} \exp\left[-\frac{1}{\sigma^2}\|\mathbf{a} - \mathbf{m}_a\|^2\right].$$

Substituting the previous three expressions into Eq. (22), we get

$$p_{\hat{c},\hat{s}}(\mathbf{w}) = \frac{1}{\gamma\pi^2\sigma^4} \iint_{-\infty}^{\infty} \exp\left[-\frac{\|\mathbf{w} - \mathbf{M}\mathbf{a}\|^2}{\gamma\sigma^2\|\mathbf{a}\|^2}\right] \exp\left[-\frac{1}{\sigma^2}\|\mathbf{a} - \mathbf{m}_a\|^2\right] \frac{d\mathbf{a}}{\|\mathbf{a}\|^2}, \tag{23}$$

where the rows of the matrix $\mathbf{M}$ are formed from $\mathbf{m}_c^T$ and $\mathbf{m}_s^T$:

$$\mathbf{M} = B\begin{pmatrix} \cos\beta\cos\psi & \cos\beta\sin\psi \\ \sin\beta\cos\psi & \sin\beta\sin\psi \end{pmatrix}.$$

Equation (23) is complicated, and we set about simplifying it.

One unsettling point is the presence of the phase ψ in Eq. (23) (through $\mathbf{m}_a$ and $\mathbf{M}$). Since the time segment over which the processing is done has no *a priori* relationship to

the phase of the input signal, ψ is unknown in practice. A good bearing estimator should not depend on ψ, and it is therefore to be hoped that ψ can somehow be eliminated from the equations. One clue about how to proceed comes from the observation that $\det \mathbf{M} = 0$; i.e., $\mathbf{M}$ is singular. In fact, $\mathbf{M}$ has unity rank, and so $\mathbf{Ma}$ in Eq. (23) traces out a line in the plane even though $\mathbf{a}$ is two dimensional. By rotating the coordinate system such that one axis is parallel to this line, one coordinate is eliminated. To this end, define a new variable of integration $\mathbf{u} = (u_1, u_2)^T$ by the linear transformation $\mathbf{a} = \mathbf{Ru}$, where the matrix $\mathbf{R}$ rotates by the angle ψ:

$$\mathbf{R} = \begin{pmatrix} \cos\psi & -\sin\psi \\ \sin\psi & \cos\psi \end{pmatrix}.$$

Since $\mathbf{R}$ is a rotation, $d\mathbf{a} = d\mathbf{u}$ and $\|\mathbf{a}\|^2 = \|\mathbf{u}\|^2$, and the integral of Eq. (23) becomes

$$p_{\hat{c},\hat{s}}(\mathbf{w}) = \frac{1}{\gamma\pi^2\sigma^4} \iint_{-\infty}^{\infty} \exp\left[-\frac{\|\mathbf{w} - \mathbf{MRu}\|^2}{\gamma\sigma^2\|\mathbf{u}\|^2}\right] \exp\left[-\frac{1}{\sigma^2}\|\mathbf{Ru} - \mathbf{m}_o\|^2\right] \frac{d\mathbf{u}}{\|\mathbf{u}\|^2}.$$

Writing the transformed terms in component form, we find

$$\mathbf{MRu} = Bu_1 \begin{pmatrix} \cos\beta \\ \sin\beta \end{pmatrix}$$

and

$$\|\mathbf{Ru} - \mathbf{m}_a\|^2 = ((u_1 - B)^2 + u_2^2).$$

The phase angle ψ has indeed been eliminated from the equations, and it follows that bearing estimates formed from $\hat{c}$ and $\hat{s}$ are unaffected by the phase of the input signal relative to the observation window. The effect of the rotation has been to concentrate the signal in the u_1 dimension, whereas the u_2 dimension corresponds to noise alone.

The next step is to switch the Cartesian coordinates $\hat{c} = w_1$ and $\hat{s} = w_2$ to polar coordinates $\hat{r}$ and $\hat{\beta}$ via Eq. (15), repeated here in the form

$$w_1 = \hat{r}\cos\hat{\beta}$$
$$w_2 = \hat{r}\sin\hat{\beta}.$$

The joint probability density function of $\hat{r}$ and $\hat{\beta}$ is given by

$$p(\hat{r}, \hat{\beta}) = |J| \cdot p_{\hat{c},\hat{s}}(\hat{r}\cos\hat{\beta}, \hat{r}\sin\hat{\beta}),$$

where the Jacobian of the coordinate transformation is $|J| = \hat{r}$. Carrying out the transformation and rearranging, we find that

$$p(\hat{r}, \hat{\beta}) = \frac{\hat{r}}{\gamma\pi^2\sigma^4} \iint_{-\infty}^{\infty} \exp\left[\frac{-1}{\gamma\sigma^2\|\mathbf{u}\|^2}(\hat{r}^2 + B^2u_1^2 - 2Bu_1\hat{r}\cos(\hat{\beta} - \beta))\right] \times \exp\left[-\frac{1}{\sigma^2}((u_1 - B)^2 + u_2^2)\right] \frac{d\mathbf{u}}{\|\mathbf{u}\|^2}. \tag{24}$$

It is now possible to find the pdf $p(\hat{\beta})$ of the bearing estimator by integrating out the unwanted variable $\hat{r}$, but the explicit formula will not be worked out. In the special case when $B = 0$ (noise only), it can be shown that $\hat{r}$ and $\hat{\beta}$ are independent and that $\hat{\beta}$ is uniformly distributed.

Even without working out the explicit form for $p(\hat{\beta})$, an important conclusion may be drawn from Eq. (24), which shows that the true bearing β and its estimate $\hat{\beta}$ will appear in the expression for $p(\hat{\beta})$ only in the form $\cos(\hat{\beta} - \beta)$. As the cosine is an even function, it follows that the pdf $p(\hat{\beta})$ is symmetric about the true value β when viewed on the unit circle. Hence the estimator is unbiased on the circle. This result can be disguised by the fact that, in computing the mean of $\hat{\beta}$, we break the circle at some point* and use a specific interval of length 2π. Suppose, for example, that the interval $[0, 2\pi)$ is chosen. As the SNR decreases, $p(\hat{\beta})$ approaches a uniform pdf and the mean of $\hat{\beta}$ approaches the mid-point of the interval, i.e., $E\{\hat{\beta}\} \to \pi$. However, $p(\hat{\beta})$ is always symmetric about β, and hence we want to choose the interval such that $E\{\hat{\beta}\} = \beta$ for all SNRs. The correct choice of interval is then $[\beta - \pi, \beta + \pi)$. Without loss of generality it will be assumed that $\beta = 0$, so that $\hat{\beta} \in [-\pi, \pi)$ and $E\{\hat{\beta}\} = 0$.

The variance $\sigma_{\hat{\beta}}^2$ of the estimator $\hat{\beta}$ is found from the equation

$$\sigma_{\hat{\beta}}^2 = \int_{-\pi}^{\pi} \int_{0}^{\infty} \hat{\beta}^2 \, p(\hat{r}, \hat{\beta}) \, d\hat{r} \, d\hat{\beta}. \tag{25}$$

Substitution of Eq. (24) into the integral (25) yields, after interchanging the order of integration and performing some simple reductions,

$$\sigma_{\hat{\beta}}^2 = \frac{1}{\pi\sigma^2} \iint_{-\infty}^{\infty} K(\zeta) \exp\Big[-\frac{1}{\sigma^2}\big((u - B)^2 + v^2\big)\Big] du \, dv, \tag{26}$$

where $K(\cdot)$ is the function defined in Eq. (17) and

$$\zeta \equiv \frac{1}{\sigma\sqrt{\gamma}} \frac{Bu}{\sqrt{u^2 + v^2}}.$$

This equation can be simplified by switching to polar coordinates. However, this is a convenient point in the discussion to introduce the more general result for multiple blocks.

A.2 Extension to Multiple Data Blocks

The previous results can be extended to the case when M blocks are integrated before forming the bearing estimate. Most of the equations are modified by replacing

* This aspect of the analysis has been the subject of some discussion in the literature; see, for example, Refs. 7, 8.

the vectors and matrices appearing therein by block vectors and matrices of M times the dimension; the derivation technique remains largely unchanged. It is found that Eq. (26) generalizes to

$$\sigma_{\hat{\beta}}^2 = \frac{1}{(\pi\sigma^2)^M} \int_{\mathbf{R}^M} \int_{\mathbf{R}^M} K(\zeta) \exp\Big[-\frac{1}{\sigma^2}(\|\mathbf{u}-\mathbf{b}\|^2 + \|\mathbf{v}\|^2)\Big] d\mathbf{u}\, d\mathbf{v}, \tag{27}$$

where now

$$\zeta = \frac{1}{\sigma\sqrt{\gamma}} \frac{\mathbf{b}^T\mathbf{u}}{\{\|\mathbf{u}\|^2 + \|\mathbf{v}\|^2\}^{1/2}}. \tag{28}$$

In Eq. (27), $\mathbf{R}$ denotes the real line, and the two integrals over $\mathbf{R}^M$ are M-fold integrals over the dummy variables of integration $\mathbf{u} = (u_1, \ldots, u_M)^T$ and $\mathbf{v} = (v_1, \ldots, v_M)^T$.

Equation (27) as it stands is not very useful for numerical work. The amount of computation required to numerically evaluate a multi-dimensional integral increases exponentially with the dimension (assuming a quadrature product rule), and the author's experience is that one cannot expect to evaluate integrals of dimension greater than about six. Formula (27) would then be useful for a maximum of two or three blocks. However, a sequence of coordinate transformations can be used to reduce Eq. (27) to a double integral, and this reduction is now discussed. A fair amount of trial and error was required before the following transformations were discovered.

The first substitution was suggested by the fact that $\mathbf{v}$ appears in Eqs. (27) and (28) only as $\|\mathbf{v}\|^2 = \sum_m v_m^2$. We therefore employ a multi-dimensional spherical transformation of coordinates where $v = \|\mathbf{v}\|$ is the radius:

$$\begin{aligned}
v_1 &= v\cos\theta_1 \\
v_2 &= v\sin\theta_1\cos\theta_2 \\
v_3 &= v\sin\theta_1\sin\theta_2\cos\theta_3 \\
&\vdots \\
v_{M-1} &= v\sin\theta_1\cdots\sin\theta_{M-2}\cos\theta_{M-1} \\
v_M &= v\sin\theta_1\cdots\sin\theta_{M-2}\sin\theta_{M-1},
\end{aligned} \tag{29}$$

where $0 \le v < \infty$, $0 \le \theta_1 \le 2\pi$, and $0 \le \theta_m \le \pi$ for $m = 2, \ldots, M-1$. It can be shown that the differential of integration becomes

$$d\mathbf{v} = v^{M-1}\sin^{M-2}\theta_1 \sin^{M-3}\theta_2 \cdots \sin\theta_{M-2}\, dv\, d\theta_1 \cdots d\theta_{M-1}.$$

Making this substitution in Eqs. (27) and performing the integrations over angle yields the formula

$$\sigma_{\hat{\beta}}^2 = \frac{2}{(\sqrt{\pi}\sigma^2)^M \Gamma(\frac{M}{2})} \int_{\mathbf{R}^M} \int_0^\infty K(\zeta) \exp\Big[-\frac{1}{\sigma^2}(\|\mathbf{u}-\mathbf{b}\|^2 + v^2)\Big] v^{M-1}\, dv\, d\mathbf{u}, \tag{30}$$

where

$$\zeta = \frac{1}{\sigma\sqrt{\gamma}} \frac{\mathbf{b}^T\mathbf{u}}{\{\|\mathbf{u}\|^2 + v^2\}^{1/2}}. \tag{31}$$

The dimensionality has been reduced from $2M$ in Eq. (27) to $M+1$ in Eq. (30). This reduction almost doubles the range of M that can be handled numerically, and Eq. (30) was used to evaluate $\sigma_{\hat{\beta}}^2$ for values of M up to 5 (before the subsequent transformations were discovered).

Transforming the variables u_m in the same way that the v_m were transformed via Eq. (29) does not lead to a simple result, because the u_m appear in the integrand in forms other than just $\|\mathbf{u}\|^2 = \sum_m u_m^2$. However, looking at Eqs. (30) and (31) and noting that

$$\|\mathbf{u} - \mathbf{b}\|^2 = \|\mathbf{u}\|^2 - 2\mathbf{b}^T\mathbf{u} + \|\mathbf{b}\|^2,$$

we see that the u_m appear only in the linear and quadratic forms $\mathbf{b}^T\mathbf{u}$ and $\|\mathbf{u}\|^2$. Let us perform a linear transformation $\mathbf{x} = \mathcal{O}\mathbf{u}$, where $\mathcal{O}$ is an $M \times M$ orthogonal matrix with first row given by $\mathbf{b}^T/\|\mathbf{b}\|$. Such a matrix can always be constructed by starting with this row, and then applying the Gram-Schmidt procedure[9] to another $M-1$ linearly independent vectors. For $\mathcal{O}$ chosen in this manner, we have $\mathbf{b}^T\mathbf{u} = \|\mathbf{b}\|x_1$ and $\|\mathbf{u}\|^2 = \|\mathbf{x}\|^2$, where the last equation follows because $\mathcal{O}^T\mathcal{O}$ is the identity matrix. The effect of the transformation has been to leave the quadratic form intact, but to simplify the linear form to a single coordinate of the new coordinate system. Also, since $\mathcal{O}$ is orthogonal, it follows that $d\mathbf{u} = d\mathbf{x}$.

Applying this transformation to the integral in Eq. (30) yields

$$\sigma_{\hat{\beta}}^2 = \frac{2e^{-\rho}}{(\sqrt{\pi}\sigma^2)^M \Gamma(\frac{M}{2})} \int_{\mathbf{R}^M} \int_0^\infty K(\zeta) \exp\Big[-\frac{1}{\sigma^2}(\|\mathbf{x}\|^2 + v^2 - 2\|\mathbf{b}\|x_1)\Big] v^{M-1}\, dv\, d\mathbf{x} \tag{32}$$

with

$$\zeta = \sqrt{\frac{\rho}{\gamma}} \frac{x_1}{\{\|\mathbf{x}\|^2 + v^2\}^{1/2}}.$$

The dimension of the integral has not been changed, but the complexity of the integrand has been reduced as discussed above. A substantial reduction in dimension now results from a transformation similar to the one in Eq. (29):

$$\begin{aligned}
x_1 &= r\cos\theta_1 \\
x_2 &= r\sin\theta_1\cos\theta_2 \\
x_3 &= r\sin\theta_1\sin\theta_2\cos\theta_3 \\
&\vdots \\
x_M &= r\sin\theta_1\cdots\sin\theta_{M-1}\cos\theta_M \\
v &= r\sin\theta_1\cdots\sin\theta_{M-1}\sin\theta_M,
\end{aligned}$$

where $0 \le r < \infty$ and $0 \le \theta_m \le \pi$ for $m = 1, \ldots, M$. The range of the angles θ_m has been selected to give $v \ge 0$, as required in Eq. (32); furthermore, the variables have been ordered such that x_1, which appears alone in the integrand, has the simplest transformation. It can be shown that the differential of volume transforms to

$$dv\, d\mathbf{x} = r^M \sin^{M-1}\theta_1 \sin^{M-2}\theta_2 \cdots \sin\theta_{M-1}\, dr\, d\theta_1 \cdots d\theta_M.$$

Carrying out the transformation in Eq. (32), we find that only the integrals in r and θ_1 present any difficulty. The remaining $M-1$ integrals over $\theta_2, \ldots, \theta_M$ are of powers of sines and can be done explicitly to yield the constant

$$\frac{\pi^{(M-1)/2}}{4} \frac{\Gamma(M/2)}{\Gamma(M-\frac{1}{2})}.$$

Putting all these results in Eq. (32) yields the formula

$$\sigma_{\hat{\beta}}^2 = \frac{e^{-\rho}}{2\sqrt{\pi}\,\sigma^{2M}\Gamma(M-\frac{1}{2})} \int_0^{\pi} K\Big(\sqrt{\tfrac{\rho}{\gamma}}\cos\theta\Big) \sin^{2M-2}\theta \times \int_0^{\infty} \exp\Big[-\frac{1}{\sigma^2}(r^2 - 2\|\mathbf{b}\| r\cos\theta)\Big] r^{2M-1}\, dr\, d\theta,$$

where the subscript has been dropped from θ_1.

We make one last transformation, setting $r = \|\mathbf{b}\| t$, and also use the evenness of the integrand with respect to θ to extend the interval of integration to $[-\pi, \pi]$. The result is

$$\sigma_{\hat{\beta}}^2 = \frac{\rho^M e^{-\rho}}{\sqrt{\pi}\,\Gamma(M-\frac{1}{2})} \int_{-\pi}^{\pi} K\Big(\sqrt{\tfrac{\rho}{\gamma}}\cos\theta\Big) \sin^{2M-2}\theta \times \int_0^{\infty} \exp\big[-\rho(t^2 - 2t\cos\theta)\big] t^{2M-1}\, dt\, d\theta. \tag{33}$$

This equation is our main expression for the bearing variance, and is given as Eq. (16) in the body of the paper. It was used to produce all the numerical results.

A.3 Evaluation of the Inner Integral

The inner integral in Eq. (33) can be expressed in terms of

$$I_n(a,b) \equiv \int_0^{\infty} \exp(-at^2 + bt) t^{n-1} dt, \qquad (n \ge 1), \tag{34}$$

which is related to the parabolic cylinder function[10,11]. By completing the square in the exponential, it is easy to derive the special case

$$I_1(a,b) = \sqrt{\frac{\pi}{a}}\, e^{b^2/4a} P\Big(\frac{b}{\sqrt{2a}}\Big), \tag{35}$$

where $P(\cdot)$ is the cumulative normal distribution function,

$$P(x) = \frac{1}{\sqrt{2\pi}} \int_{-\infty}^{x} e^{-\frac{1}{2}t^2} dt.$$

Furthermore, it is evident from Eq. (34) that

$$\frac{\partial}{\partial b} I_n(a,b) = I_{n+1}(a,b), \tag{36}$$

and hence the higher-order formulas can be derived starting from Eq. (35). For example, differentiating Eq. (35) with respect to b yields the formula

$$I_2(a,b) = \frac{1}{2a} + \frac{b}{2a}\sqrt{\frac{\pi}{a}}\, e^{b^2/4a} P\Big(\frac{b}{\sqrt{2a}}\Big). \tag{37}$$

The expressions thus generated can be used to evaluate the inner integral in Eq. (33); in the important case of a single data block, Eq. (37) gives the formula

$$\sigma_{\hat{\beta}}^2 = \frac{1}{2\pi} \int_{-\pi}^{\pi} K\left(\sqrt{\frac{\rho}{\gamma}}\cos\theta\right) \left[e^{-\rho} + \sqrt{2\pi}\,\lambda\, e^{-\rho\sin^2\theta} P(\lambda)\right] d\theta,$$

with $\lambda \equiv \sqrt{2\rho}\cos\theta$.

The above procedure suffices for finding analytical formulas when the number of blocks M is small. However, it is not easily implemented in a computer code for evaluating $\sigma_{\hat{\beta}}^2$ when M is arbitrary, since numerical differentiation is in general poorly conditioned*. A more useful procedure stems from applying integration by parts to integral (34) to produce the recursion equation

$$I_{n+2} = \frac{1}{2a}(b\, I_{n+1} + n\, I_n) \qquad \text{for } n = 1, 2, \ldots \tag{38}$$

This formula is convenient for both analytical and numerical work. For analytical work, we start with the formulas in Eqs. (35) and (37) and use the recursion to generate higher-order formulas. For numerical work, we first evaluate I_1 and I_2 for given values of the arguments and apply Eq. (38) numerically. The recursion is far more amenable to numerical implementation than the differentiation specified in Eq. (36).

* We seek a purely numerical program, excluding the possibility of using a specialized symbolic manipulator to perform the differentiations.

APPENDIX B: HIGH-SNR APPROXIMATION FOR THE ERROR

It is possible to derive the high-SNR approximation of Eq. (18) from the second-order statistics of the noise, as will now be demonstrated for the case of a single data block. The development is terse, as the focus of this paper is on the derivation of the exact expression for the bearing variance.

We start with the formation of the components $\hat{s} = \mathrm{Re}\{X_s X_o^*\}$ and $\hat{c} = \mathrm{Re}\{X_c X_o^*\}$. Using the signal-and-noise model of Eq. (5), we have

$$\begin{aligned} X_s X_o^* &= (Be^{i\psi}\sin\beta + N_s)(Be^{-i\psi} + N_o^*) \\ &= B^2\sin\beta + Be^{-i\psi}N_s + Be^{i\psi}N_o^*\sin\beta + N_s N_o^*. \end{aligned} \tag{39}$$

The phasors $e^{\pm i\psi}$ can be absorbed into the complex Gaussian noise without changing the statistics; i.e., the equation

$$X_s X_o^* = B^2\sin\beta + B\,N_s + B\,N_o^*\sin\beta + N_s N_o^*$$

is statistically equivalent to Eq. (39). For high SNR, the quadratic term in the noise can be omitted to yield

$$X_s X_o^* \cong B^2\sin\beta + B(N_s + N_o^*\sin\beta).$$

A similar development can be used for $X_c X_o^*$, leading to the result

$$\frac{\hat{s}}{\hat{c}} \cong \frac{B^2\sin\beta + B(N_{s,r} + N_{o,r}\sin\beta)}{B^2\cos\beta + B(N_{c,r} + N_{o,r}\cos\beta)},$$

where $N_{o,r} \equiv \mathrm{Re}\{N_o\}$, etc. It will be assumed that $\sin\beta \neq 0$ and $\cos\beta \neq 0$; the special cases when the sine or cosine is zero can be handled separately and yield the same result. The previous equation may then be re-written as

$$\frac{\hat{s}}{\hat{c}} \cong \left(\frac{1+a}{1+b}\right)\tan\beta, \tag{40}$$

where

$$a \equiv \frac{1}{B}\left(\frac{N_{s,r}}{\sin\beta} + N_{o,r}\right) \quad \text{and} \quad b \equiv \frac{1}{B}\left(\frac{N_{c,r}}{\cos\beta} + N_{o,r}\right). \tag{41}$$

When the SNR is large, $|a| \ll 1$ and $|b| \ll 1$, and

$$\frac{1+a}{1+b} \cong (1+a)(1-b) = 1 + a - b + ab \cong 1 + a - b. \tag{42}$$

Applying approximation (42) to Eq. (40) and using Eq. (41), we obtain

$$\hat{s}/\hat{c} \cong (1+\epsilon)\tan\beta$$

with

$$\epsilon \equiv \frac{1}{B}\left(\frac{N_{s,r}}{\sin\beta} - \frac{N_{c,r}}{\cos\beta}\right). \tag{43}$$

The bearing estimate is given by

$$\hat{\beta} = \arctan(\hat{s}/\hat{c}) \cong \arctan\left((1+\epsilon)\tan\beta\right),$$

or, to first order in the small quantity ϵ,

$$\hat{\beta} \cong \beta + \epsilon \sin\beta\cos\beta.$$

The variance of the bearing estimate is then approximated by

$$\sigma_{\hat{\beta}}^2 \cong \sigma_\epsilon^2 \sin^2\beta\cos^2\beta. \tag{44}$$

From the covariance matrix in Eq. (6) it follows that $N_{s,r}$ and $N_{c,r}$ each have variance $\frac{1}{2}\gamma\sigma^2$; the use of Eq. (43) in Eq. (44) then yields the final approximation

$$\begin{aligned}\sigma_{\hat{\beta}}^2 &\cong \frac{\gamma\sigma^2}{2B^2}\left(\frac{1}{\sin^2\beta} + \frac{1}{\cos^2\beta}\right)\sin^2\beta\cos^2\beta \\ &= \frac{\gamma}{2\rho},\end{aligned}$$

where $\rho = B^2/\sigma^2$ is the SNR as defined in the main body of the paper. This last result is the high-SNR approximation we sought to derive.

REFERENCES

1. H. Merklinger, private communication.
2. S.W. Davies, "Arctan bearing estimators," in Proc. Thirteenth Biennial Symposium on Communications, held June 1986 at Queen's University, Kingston, ON, pp. B.4.5–B.4.8.
3. S.W. Davies, "Bearing accuracies for arctan processing of crossed dipole arrays," in Proc. Oceans '87, held 28 Sept – 1 Oct 1987 in Halifax, NS, vol. 1, pp. 351–356.
4. R.S. Walker, "The detection performance of FFT processors for narrowband signals," Technical Memorandum 82/A, Defence Research Establishment Atlantic, 1982.
5. L.L. Scharf, *Statistical Signal Processing: Detection, Estimation, and Time Series Analysis.* Reading, Mass: Addison-Wesley, 1991.
6. W.R. Bennett and J.R. Davey, *Data Transmission.* New York: McGraw-Hill, 1965.
7. M. Kendall and A. Stuart, *The Advanced Theory of Statistics.* Vol. 1, *Distribution Theory.* 4th edition, New York: MacMillan, 1977. (See §5.33)
8. See: S.M. Kay, "Comments on 'Frequency Estimation by Linear Prediction'", IEEE Trans. on Acoustics, Speech, and Signal Processing, vol. ASSP-27, April 1979, pp. 198–199, and the reply by L.B. Jackson and D.W. Tufts on p. 200 of the same issue.
9. P.J. Davis, *Interpolation and Approximation.* New York: Dover, 1975.
10. E.T. Whittaker and G.N. Watson, *A Course in Modern Analysis.* Cambridge University Press, 1922.
11. I.S. Gradshteyn and I.M. Ryzhik, *Table of Integrals, Series, and Products.* San Diego: Academic Press, 1980.

UNCLASSIFIED
SECURITY CLASSIFICATION OF FORM
(highest classification of Title, Abstract, Keywords)

DOCUMENT CONTROL DATA

(Security classification of title, body of abstract and indexing annotation must be entered when the overall document is classified)

1. ORIGINATOR (the name and address of the organization preparing the document.. Organizations for whom the document was prepared, e.g. Establishment sponsoring a contractor's report, or tasking agency, are entered in section 8.)

Defence Research Establishment Atlantic
PO Box 1012
Dartmouth, Nova Scotia, Canada B2Y 3Z7

2. SECURITY CLASSIFICATION (overall security classification of the document including special warning terms if applicable).

UNCLASSIFIED

3. TITLE (the complete document title as indicated on the title page. Its classification should be indicated by the appropriate abbreviation (S,C,R or U) in parentheses after the title).

The Performance of the Arctangent Bearing Estimator in Isotropic Noise (U)

4. AUTHORS (Last name, first name, middle initial. If military, show rank, e.g. Doe, Maj. John E.)

Maranda, Brian H.

5. DATE OF PUBLICATION (month and year of publication of document)

September 1999

6a. NO .OF PAGES (total containing information Include Annexes, Appendices, etc).

28

6b. NO. OF REFS (total cited in document)

11

7. DESCRIPTIVE NOTES (the category of the document, e.g. technical report, technical note or memorandum. If appropriate, enter the type of report, e.g. interim, progress, summary, annual or final. Give the inclusive dates when a specific reporting period is covered).

TECHNICAL MEMORANDUM

8. SPONSORING ACTIVITY (the name of the department project office or laboratory sponsoring the research and development. Include address).

Defence Research Establishment Atlantic

9a. PROJECT OR GRANT NO. (if appropriate, the applicable research and development project or grant number under which the document was written. Please specify whether project or grant).

Project 1cc11

9b. CONTRACT NO. (if appropriate, the applicable number under which the document was written).

10a ORIGINATOR'S DOCUMENT NUMBER (the official document number by which the document is identified by the originating activity. This number must be unique to this document.)

DREA Technical Memorandum 1999-145

10b OTHER DOCUMENT NOs. (Any other numbers which may be assigned this document either by the originator or by the sponsor.)

11. DOCUMENT AVAILABILITY (any limitations on further dissemination of the document, other than those imposed by security classification)

(X) Unlimited distribution
( ) Defence departments and defence contractors; further distribution only as approved
( ) Defence departments and Canadian defence contractors; further distribution only as approved
( ) Government departments and agencies; further distribution only as approved
( ) Defence departments; further distribution only as approved
( ) Other (please specify):

12. DOCUMENT ANNOUNCEMENT (any limitation to the bibliographic announcement of this document. This will normally correspond to the Document Availability (11). However, where further distribution (beyond the audience specified in (11) is possible, a wider announcement audience may be selected).

UNCLASSIFIED
SECURITY CLASSIFICATION OF FORM

13. ABSTRACT (a brief and factual summary of the document. It may also appear elsewhere in the body of the document itself. It is highly desirable that the abstract of classified documents be unclassified. Each paragraph of the abstract shall begin with an indication of the security classification of the information in the paragraph (unless the document itself is unclassified) represented as (S), (C), (R), or (U). It is not necessary to include here abstracts in both official languages unless the text is bilingual).

One well-known system for estimating the bearing to an underwater acoustic source consists of two crossed dipoles and an omni-directional hydrophone. The bearing is computed from the sensor data using an estimator based on the arctangent function. In this paper, the performance of the arctan bearing estimator is examined for a sinusoidal signal in isotropic Gaussian noise. It is shown analytically that the estimator is unbiased, and an exact formula for the bearing variance is derived; this formula is valid for an arbitrary number of data blocks and arbitrary values of the signal-to-noise ratio (SNR). Numerical examples show that the variance of the arctan estimator approaches the Cramer-Rao lower bound for high SNRs, and the threshold region below which the bearing accuracy degrades rapidly is clearly identified. Two different strategies are compared for averaging multiple data blocks while forming the bearing estimate.

14. KEYWORDS, DESCRIPTORS or IDENTIFIERS (technically meaningful terms or short phrases that characterize a document and could be helpful in cataloguing the document. They should be selected so that no security classification is required. Identifiers, such as equipment model designation, trade name, military project code name, geographic location may also be included. If possible keywords should be selected from a published thesaurus. e.g. Thesaurus of Engineering and Scientific Terms (TEST) and that thesaurus-identified. If it not possible to select indexing terms which are Unclassified, the classification of each should be indicated as with the title).

Accuracy
Arctangent
Bearing
Dipoles
Localization
Variance

DCD03 2/06/87-M/ DREA mod. 17 Dec 1997